



A Four-Gene-Based Prognostic Model Predicts Overall Survival in Patients With Cutaneous Melanoma

Xiaoxia Tong^{1,2†}, Xiaofei Qu^{1,2†} and Mengyun Wang^{1,2*}

¹ Cancer Institute, Fudan University Shanghai Cancer Center, Shanghai, China, ² Department of Oncology, Shanghai Medical College, Fudan University, Shanghai, China

OPEN ACCESS

Edited by:

Wen-Qing Li,
Peking University Cancer Hospital,
China

Reviewed by:

Yun Hak Kim,
Pusan National University,
South Korea
Ioana Cosgarea,
Newcastle University, United Kingdom

*Correspondence:

Mengyun Wang
wangmengyun@fudan.edu.cn

[†]These authors have contributed
equally to this work

Specialty section:

This article was submitted to
Skin Cancer,
a section of the journal
Frontiers in Oncology

Received: 24 December 2020

Accepted: 29 January 2021

Published: 24 March 2021

Citation:

Tong X, Qu X and Wang M (2021) A
Four-Gene-Based Prognostic Model
Predicts Overall Survival in Patients
With Cutaneous Melanoma.
Front. Oncol. 11:639874.
doi: 10.3389/fonc.2021.639874

Background: Cutaneous melanoma (CM) is one of the most aggressive cancers with highly metastatic ability. To make things worse, there are limited effective therapies to treat advanced CM. Our study aimed to investigate new biomarkers for CM prognosis and establish a novel risk score system in CM.

Methods: Gene expression data of CM from Gene Expression Omnibus (GEO) datasets were downloaded and analyzed to identify differentially expressed genes (DEGs). The overlapped DEGs were then verified for prognosis analysis by univariate and multivariate COX regression in The Cancer Genome Atlas (TCGA) datasets. Based on the gene signature of multiple survival associated DEGs, a risk score model was established, and its prognostic and predictive role was estimated through Kaplan-Meier (K-M) analysis and log-rank test. Furthermore, the correlations between prognosis related genes expression and immune infiltrates were analyzed via Tumor Immune Estimation Resource (TIMER) site.

Results: A total of 103 DEGs were obtained based on GEO cohorts, and four genes were verified in TCGA datasets. Subsequently, four genes (*ADAMDEC1*, *GNLY*, *HSPA13*, and *TRIM29*) model was developed by univariate and multivariate Cox regression analyses. The K-M plots showed that the high-risk group was associated with shortened survival than that in the low-risk group ($P < 0.0001$). Multivariate analysis suggested that the model was an independent prognostic factor (high-risk vs. low-risk, HR= 2.06, $P < 0.001$). Meanwhile, the high-risk group was prone to have larger breslow depth ($P < 0.001$) and ulceration ($P < 0.001$).

Conclusions: The four-gene risk score model functions well in predicting the prognosis and treatment response in CM and will be useful for guiding therapeutic strategies for CM patients. Additional clinical trials are needed to verify our findings.

Keywords: prognosis, cutaneous melanoma, risk score, gene signature, survival

INTRODUCTION

Cutaneous melanoma (CM) accounts for over 74% of skin cancer related death each year (1), which makes it one of the most malignant cancers, with tremendously poor prognosis (2, 3). The incidence of CM has continued to increase annually. Although tremendous efforts toward early detection and therapeutics were made, advanced stage melanoma patients still exhibit disappointing prognosis with 5-year overall survival rate ranging from 45% for stage III to 18% for stage IV (4, 5).

Cutaneous melanoma is a highly heterogeneous tumor, in terms of clinical and complicated molecular (5). Several clinical features, such as age, gender, stage, ulceration and breslow thickness have been shown to be the important clinicopathological characteristics for predicting the outcome of CM patient (6). However, due to the high potentiality for CM metastasis, the prognosis remains poor. Molecular biomarkers are important in guiding treatment selection and predicting outcome in tumor patients (7–9). For example, the 21-gene recurrence score assay is prognostic for women with node-negative, estrogen-receptor-positive breast cancer treated with tamoxifen (10). Although hundreds of studies have explored the prognostic value of molecular markers, there is still no recommended molecular marker to predict CM prognosis.

In the current study, we were devoted to exploring new biomarkers and establishing a risk score model to predict prognosis, aiming to provide appropriate therapeutic methods for CM patients.

MATERIALS AND METHODS

Gene Expression Omnibus (GEO) Datasets Collection and Enrichment Analysis

Gene expression raw microarray cell intensity (CEL) profiles of CM were evaluated in three independent datasets from the GEO database (accession number: GSE7553, GSE46517, and GSE15605), which included 57 tumor tissue samples and three normal skin samples; 85 tumor tissue samples and eight normal skin samples; 60 tumor tissue samples and six normal skin samples, respectively. The microarray data GSE65904 containing 214 patients was downloaded to verify our risk model. Four patients were deleted due to lack of follow-up information. When more than one probe matched the same gene ID, the mean expression value of the gene was used for our study.

The Cancer Genome Atlas (TCGA) Dataset

The TCGA CM dataset, containing 459 tumor samples which included raw counts of RNAseq expression data and clinicopathological characteristics were obtained from cBioPortal website. The TCGA dataset was randomly divided into two parts: the training cohort and the validation cohort.

Identification of Common Differential Expression Genes (DEG)

The GSE7553, GSE46517, and GSE15605 expression profiles were normalized and the DEG were calculated using the LIMMA package. In this study, Gene sets with False Discovery Rate (FDR) < 0.05 and with the threshold of $|\log_{2}FC| > 1$ were defined as DEGs. All the data processing and normalization were performed using the R software.

Identification and Selection of Prognosis-Related Genes

Univariate and multivariate Cox regression analyses model were commonly employed in survival analysis. Genes were considered significant when the *P* value were <0.05 in the univariate and multivariate Cox regression analysis based on training and validation cohorts. These genes were used to construct the risk model. The fitness of the models was compared based on Akaike information criterion (AIC) and the lowest value of AIC provided the sensitivity and specificity. Subsequently, four genes (*ADAMDEC1*, *GNLY*, *HSPA13*, and *TRIM29*) were selected.

Construction and Assessment of Risk Score System

Based on the prognosis associated genes, a risk score model was constructed for the CM patients. Each gene was added one at a time in the risk score system and the risk score for each patient was calculated as the sum of each gene's score as follows:

$$\text{Risk score} = \beta_{\text{gene1}} * \text{Exp gene1} + \beta_{\text{gene2}} * \text{Exp gene2} + \dots + \beta_{\text{gene}(n)} * \text{Exp gene}(n)$$

In this formula, $\beta_{\text{gene}(n)}$ represents the coefficient of each gene from univariate Cox regression analysis, and $\text{Exp gene}(n)$ displays the expression of each gene.

Then all TCGA patients were separated into high and low-risk subgroups according to the optimal cut-off value of risk score. The optimal cut-off value of risk score was determined by the time-dependent receiver operating characteristic (ROC) curve using “survivalROC” package. To compare the survival time difference between the low- and high-risk group, K-M curve was produced by the “Survminer” package using the log-rank test. The predictive accuracy of this risk score model was determined by time-dependent ROC curve analysis. The area under the curve (AUC) was calculated to measure the predictive ability of the gene signature for clinical outcomes.

Immune Infiltration Analysis

The abundance of tumor infiltrating immune cells in CM was predicted using the Tumor Immune Estimation Resource (TIMER) algorithm. The correlation between prognostic gene expression and the abundance of different immune cells, including CD8+ T cells, CD4+ T cells, macrophages, B cells, neutrophils, and dendritic cells was measured using the

Spearman's test. All hypothetical tests were two-sided and P values < 0.05 were considered statistically significant.

RESULTS

Screening of DEG

To describe our study more clearly, a flow chart of the analysis procedure was developed (Figure 1). After the analyses of GSE7553, GSE46517, and GSE15605 data sets, DEGs were identified and selected. The overlap among three data sets included 103 DEGs was shown in the Venn diagram (Figure 2A). The volcano plots and heatmap of each data set are shown in Figures 2B–G.

Construction of Risk Score System

We conducted univariate and multivariate Cox regression to investigate the correlation of the DEGs with the overall survival of TCGA CM patients in training, validation and total cohort. Basic characteristics of the patients are shown in Table 1. The

result revealed that *GNLY*, *DFNA28*, *ADAMDEC1*, *ALOXE3*, *EFNA3*, *EPN3*, *EVPL*, *FERMT1*, *HSPA13*, *JAG2*, *RAPGEFL1*, *SULT2B1*, *TGM3*, and *TRIM29* were significant prognostic factors. Furthermore, in order to select the best performance efficacy predictive model with the lowest AIC value, we performed the stepwise multivariate Cox regression analysis to identify independent predictors for overall survival of total TCGA CM patients. Finally, four prognosis-associated genes (*GNLY*, *ADAMDEC1*, *HSPA13*, and *TRIM29*) were selected for constructing the risk score system (Table 2). The formula was as follows:

$$\text{Risk score} = (-0.101) * \text{ExpADAMDEC1} + (-0.091) * \text{ExpGNLY} + (-0.284) * \text{ExpHSPA13} + 0.102 * \text{ExpTRIM29}$$

To evaluate the prognostic significance of the risk score, K-M plot of high and low risk CM patients were conducted. According to the optimal cut-off value of risk score, the patients in the total TCGA cohort were classified into high (312 patients) and low (147 patients) risk groups. Compared to the high-risk group with the median OS time of 27.76 months,

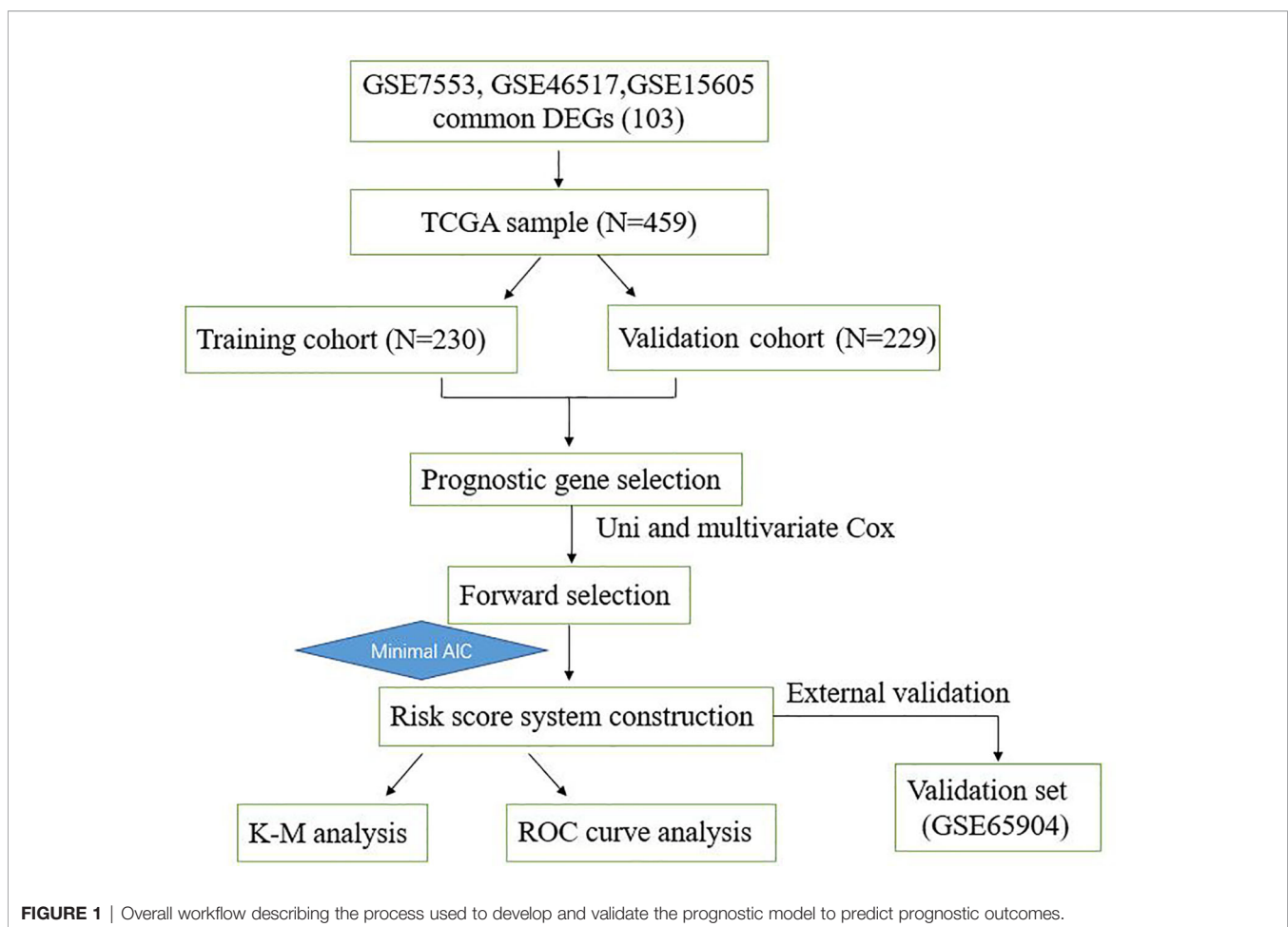


FIGURE 1 | Overall workflow describing the process used to develop and validate the prognostic model to predict prognostic outcomes.

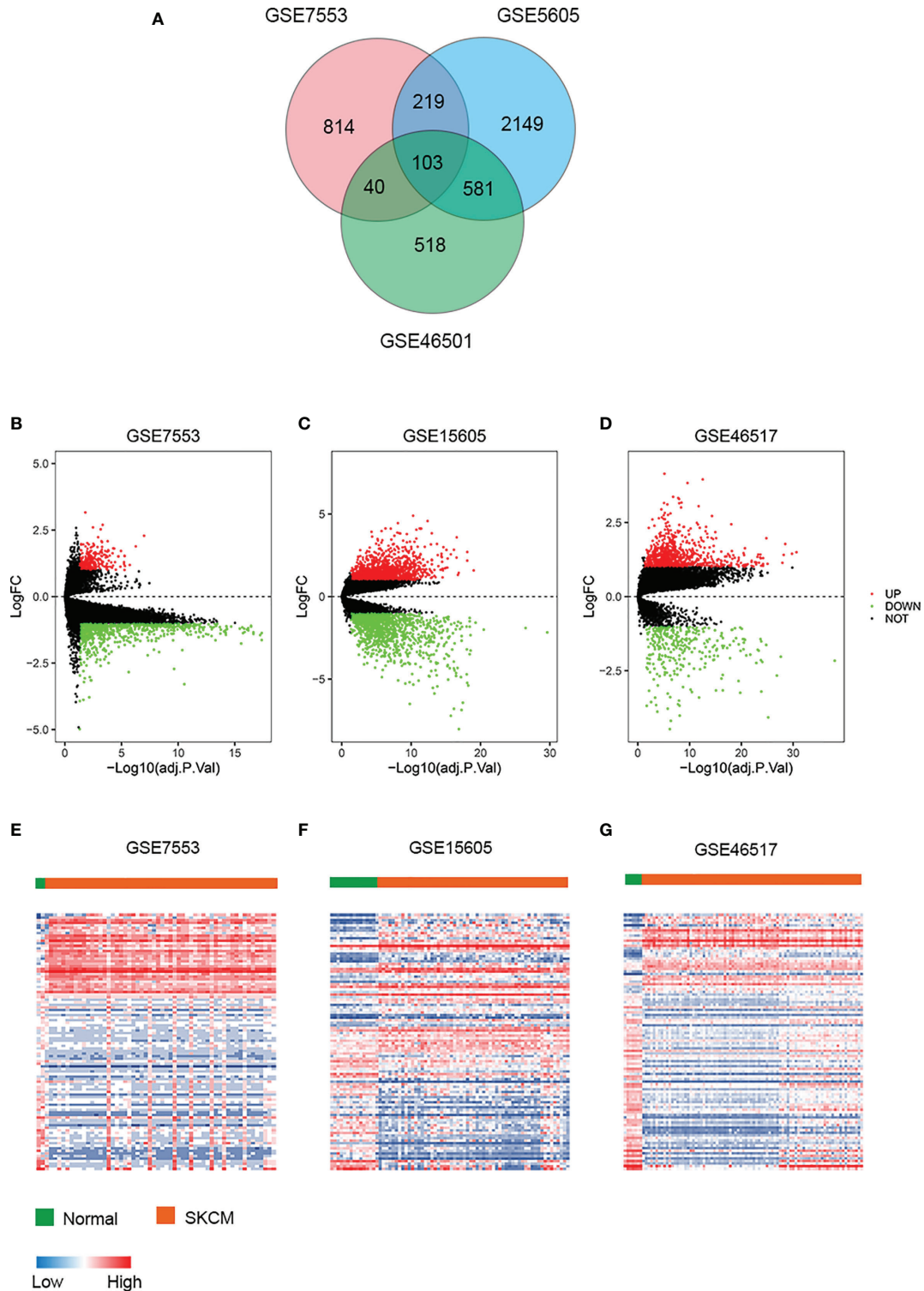


FIGURE 2 | DEGs in three data sets. **(A)** Venn diagram of DEGs. **(B–D)** The volcano plots visualize the DEGs in GSE7553, GSE15605, and GSE46517, respectively. The red nodes represent upregulated genes. The green nodes represent downregulated genes. **(E–G)** Heatmap of the top 103 DEGs according to the value of $|\log\text{FC}| > 1$ and $\text{FDR} < 0.05$. The color in heat maps from blue to red shows the progression from low expression to high expression. $\log\text{FC}$, log fold change.

TABLE 1 | Basic characteristics of TCGA CM patients.

Characteristics	Groups	Total (N=459)		Training cohort (N=229)		Validation cohort (N=230)	
		No	%	No	%	No	%
Age	≤58	233	50.7	116	50.7	117	50.9
	>58	226	49.3	113	49.3	113	49.1
Sex	Female	175	38.1	82	35.8	93	40.4
	Male	284	61.9	147	64.2	137	59.6
Metastasis	No	410	89.3	209	91.3	201	87.4
	Yes	23	5	9	3.9	14	6.1
	missing	26	5.7	11	4.8	15	6.5
Ulceration	No	145	31.6	70	30.6	75	32.6
	Yes	165	35.9	92	40.2	73	31.7
	Missing	149	32.5	67	29.2	82	35.7
Pathologic Stage	0	6	1.3	3	1.3	3	1.3
	I	77	16.8	40	17.5	37	16.1
	II	139	30.3	73	31.8	66	28.7
	III	169	36.8	81	35.4	88	38.3
	IV	22	4.8	9	4	13	5.6
	Missing	46	10	23	10	23	10
Tumor Site	Trunk	166	36.2	86	37.6	80	34.8
	Extremities	194	42.3	100	43.7	94	40.9
	Head and neck	35	7.6	15	6.5	20	8.7
	Missing	64	13.9	28	12.2	36	15.6
Breslow thickness (mm)	≤2	136	29.6	73	31.9	63	27.4
	2–5	113	24.6	52	22.7	61	26.5
	>5	105	22.9	59	25.8	46	20
	Missing	105	22.9	45	19.6	60	26.1
Chemotherapy	No	323	70.4	153	66.8	170	73.9
	Yes	88	19.2	49	21.4	39	17
	Missing	48	10.4	27	11.8	21	9.1
Radiotherapy	No	341	74.3	170	74.2	171	74.3
	Yes	73	15.9	34	14.9	39	17
	Missing	45	9.8	25	10.9	20	8.7

TABLE 2 | Univariate and multivariate analysis of prognosis genes for TCGA CM.

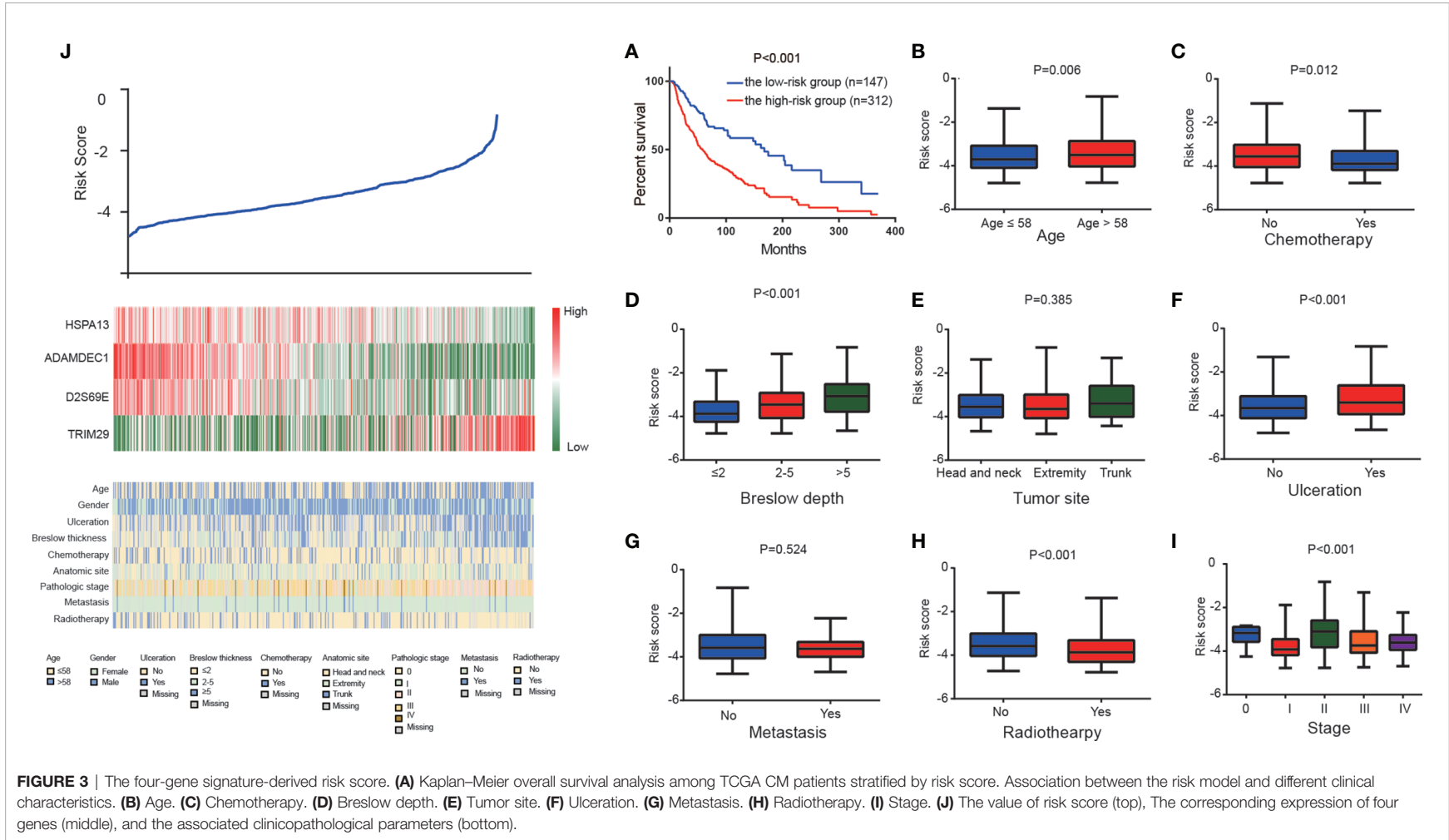
Training cohort		Univariate analysis			Multivariate analysis		
Genes	coef	HR (95%CI)	P	coef	HR (95%CI)	P	
ADAMDEC1	-0.098	0.906 (0.848–0.969)	0.004	-0.099	0.906 (0.845–0.971)	0.005	
D2S69E	-0.084	0.919 (0.847–0.998)	0.043	-0.089	0.915 (0.839–0.998)	0.045	
HSPA13	-0.346	0.708 (0.594–0.844)	0.000	-0.251	0.778 (0.648–0.936)	0.007	
TRIM29	0.088	1.092 (1.033–1.154)	0.002	0.074	1.077 (1.017–1.141)	0.011	
Validation cohort		Univariate analysis			Multivariate analysis		
Genes	coef	HR (95%CI)	P	coef	HR (95%CI)	P	
ADAMDEC1	-0.102	0.903 (0.852–0.958)	0.000	-0.113	0.893 (0.834–0.956)	0.001	
D2S69E	-0.099	0.905 (0.843–0.971)	0.006	-0.092	0.909 (0.844–0.986)	0.021	
HSPA13	-0.232	0.793 (0.637–0.987)	0.038	-0.227	0.797 (0.641–0.991)	0.042	
TRIM29	0.112	1.119 (1.066–1.174)	0.000	0.101	1.106 (1.052–1.164)	0.000	
Total		Univariate analysis			Multivariate analysis		
Genes	coef	HR (95%CI)	P	coef	HR (95%CI)	P	
ADAMDEC1	-0.101	0.905 (0.866–0.945)	0.000	-0.108	0.898 (0.857–0.940)	0.000	
D2S69E	-0.091	0.913 (0.865–0.963)	0.000	-0.093	0.911 (0.862–0.964)	0.000	
HSPA13	-0.284	0.753 (0.657–0.864)	0.000	-0.264	0.768 (0.669–0.882)	0.000	
TRIM29	0.102	1.108 (1.068–1.148)	0.000	0.091	1.095 (1.055–1.136)	0.000	

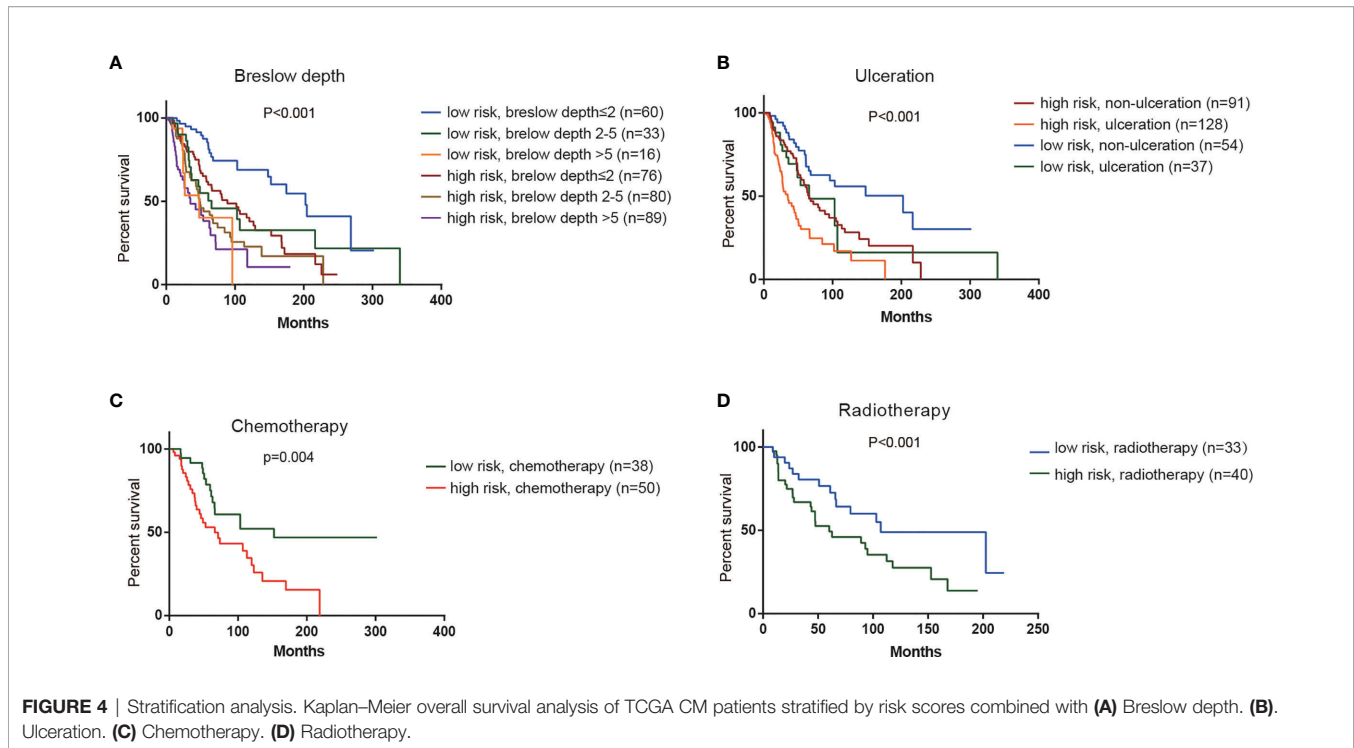
the low-risk group with the median OS time of 56.8 months had a higher survival ratio ($P < 0.001$; **Figure 3A**).

Furthermore, we analyzed the correlation between risk score and clinicopathological characteristics, which showed that high risk score was positively associated with elder age, ulceration, and breslow depth. Patients who received chemotherapy and radiotherapy prone to low-risk (**Figures 3B–J**).

Stratification Analysis

According to K-M analysis, CM patients with high risk score and larger breslow depth had the worst outcomes (**Figure 4A**), and CM patients with the ulceration and high-risk score had a shorter survival time than those with the non-ulceration group (**Figure 4B**). Furthermore, high risk score was also associated with poor prognosis in CM patients treated with chemotherapy





or radiotherapy (Figures 4C, D), indicating that the risk score could predict the therapeutic reaction.

Survival Predictive Model Based on Clinical Factors Alone or Their Combination With Risk Score

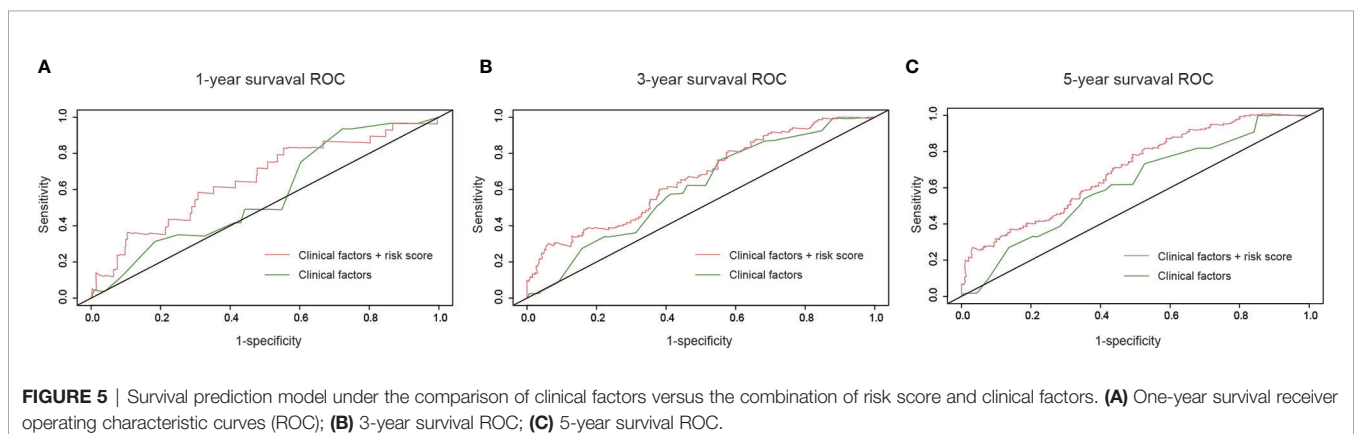
We constructed a survival prediction model to identify whether risk score in the presence of clinical factors to better discriminate survival of CM patients. Compared with the model with clinical factors alone, the model with addition of the risk score improved the sensitivity and specificity of discriminating 1-year (AUC, 0.57 to 0.66, Figure 5A), 3-year (AUC, 0.61 to 0.66, Figure 5B), and 5-year survival (AUC, 0.61 to 0.70, Figure 5C). When the model had both the risk score and clinical factors, its predictive ability for survival was greater [Concordance index (C-index) = 0.66] than that with clinical factors alone (C-index=0.59).

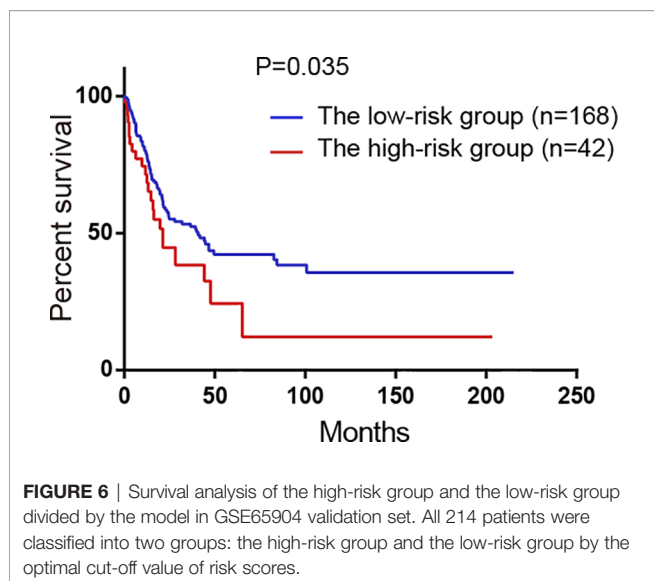
External Validation of the Model in GSE65904

GSE65904 dataset was used to validate the prediction performance of the model and each patient's risk score was calculated according to the formula of the model. All patients were divided into two groups: the high-risk group and the low-risk group by the optimal cut-off value of risk score. The K-M curve revealed significant difference in overall survival between groups in GSE65904. High-risk group had markedly poorer outcome than low-risk group with $P < 0.05$ in Figure 6.

The Association Between Prognosis Related Gene and Immune Markers

In order to detect the correlation between prognosis related gene and the immune infiltration level, we concentrated particularly on the relationship between prognosis related gene and immune





markers of various immune cells in CM using the TIMER database. There was a positive correlation between *ADAMDEC1* expression and the dendritic cell ($\text{Cor}=0.67$, $p=4.72e-59$), neutrophils ($\text{Cor}=0.652$, $p=3.99e-56$), CD8^+

T cells ($\text{Cor}=0.572$, $p=2.05e-39$), macrophages ($\text{Cor}=0.404$, $p=3.12e-19$), CD4^+ T cells ($\text{Cor}=0.385$, $p=3.45e-17$), B cells ($\text{Cor}=0.371$, $p=4.51e-16$). Similar results were obtained for *GNLY* and *HSPA13* (Figures 7A–C). While, the correlation between *TRIM29* and immune infiltration is not obvious (Figure 7D). According to K-M analysis, high *ADAMDEC1*, *HSPA13*, and *GNLY* expression was significantly correlated with better prognosis, while high *TRIM29* expression was markedly correlated with poor prognosis (Figures 7E–H).

DISCUSSION

In present study, we selected and constructed a four-gene based risk score model for CM. We analyzed GSE7553, GSE46517, and GSE15605 data sets, 103 DEGs were identified and selected. Subsequently, univariate and multivariate COX regression were employed for the key genes. Fourteen genes (*GNLY*, *DFNA28*, *ADAMDEC1*, *ALOXE3*, *EFNA3*, *EPN3*, *EVPL*, *FERMT1*, *HSPA13*, *JAG2*, *RAPGEFL1*, *SULT2B1*, *TGM3*, and *TRIM29*) were finally identified to be the prognostic genes. Here we adopted stepwise multivariate Cox regression analysis to select the best performance efficacy predictive model with the lowest AIC value. Finally, a four-gene based model including *GNLY*, *ADAMDEC1*, *HSPA13*, and *TRIM29* was successfully developed.

Furthermore, in order to evaluate the prognostic significance of the new risk model, we performed log-rank test and the ROC curve analysis to investigate association between the model and clinical parameters. As we expected, the high-risk cohort was correlated

with poor outcome and was tend to larger breslow depth and ulceration.

For our prognosis related genes, researchers have revealed that some of them may be crucial in cancer development, including CM. For instance, *ALOXE3*, which encodes arachidonate lipoxygenase3, can serve as a potential predictive biomarker for colon adenocarcinoma patients. Low expression of *ALOXE3* had a favorable prognosis of COAD (11). Gómez-Maldonado et al. identified *EFNA3*, a member of the ephrin type A ligands, is induced by hypoxia-inducible factor in human tumors and this induction is predictive of poor prognosis and increased risk of metastasis in breast cancer patients (12). *EPN3* expression is upregulated in wounded epithelial tissues and it can drive breast tumorigenesis by increasing E-cadherin endocytosis, *EPN3* is overexpressed in 40% of breast cancers and its overexpression is an independent predictor of distant metastasis (13, 14).. *Envoplakin* (*EVPL*) is a protein component of desmosomes and the DNA variant in intron of *EVPL* (*rs2071194*) has been found associated with papillary and follicular thyroid cancer risk (15). *FERMT1*, as an oncogene, promotes the degradation of $\text{I}\kappa\text{B}\alpha$, thereby activating NF- κB signaling and promoting gastric cancer (16). *JAG2* is one of Notch ligands, which recently appear to exert various carcinogenesis. *JAG2* expression significantly correlates with angiogenic processes and vascular development in breast cancer, and is induced at the transcriptional level in hypoxic tumor cells. The oncogene *c-myc* can also modulate *JAG2* expression under hypoxic conditions (17). In 2013, Takahashi et al. reported that *RAPGEFL1* was highly methylated in some ESCC cell lines and *RAPGEFL1* could regulate by most miRNAs. Therefore, *RAPGEFL1* may be the potential pathogenic genes for ESCC (18). *TGM3* could affect epithelial-mesenchymal transition, play an essential role in tumorigenesis and progression. It might serve as a useful biomarker and potential therapeutic target for hepatocellular carcinoma treatment (19).

Several genes in our risk model had been investigated in immune response. *TRIM29*, a member of the tripartite interaction motif (TRIM) family of proteins, functions as a negative regulator of innate immune response. Studies have shown that knockdown of *TRIM29* in airway epithelial cells enhances type I interferon production (20). *TRIM29* is also recognized as an oncogene, and elevated gene expression in multiple tumors such as colorectal cancer and bladder cancer and so on (21). But the function of *TRIM29* in cutaneous melanoma remained still unknown. Elizabeth et al. discovered that *ADAMDEC1*, an orphan ADAM-like metalloprotease, is expressed in the immune system, by dendritic cells and macrophages. *In vitro*, the expression of *ADAMDEC1* was significantly elevated in M1 but not M2 macrophages. More research is needed to determine the associations between *ADAMDEC1* and immune response and associations with survival for cancers (22). Granulysin (*GNLY*) is a cytolytic apoptotic molecule highly expressed in activated immune cells, particularly human cytotoxic T lymphocytes (CTLs) and natural killer (NK) cells (23). *GNLY* functions as a lytic molecule to carry out lysis or apoptosis product in target cells, including tumor

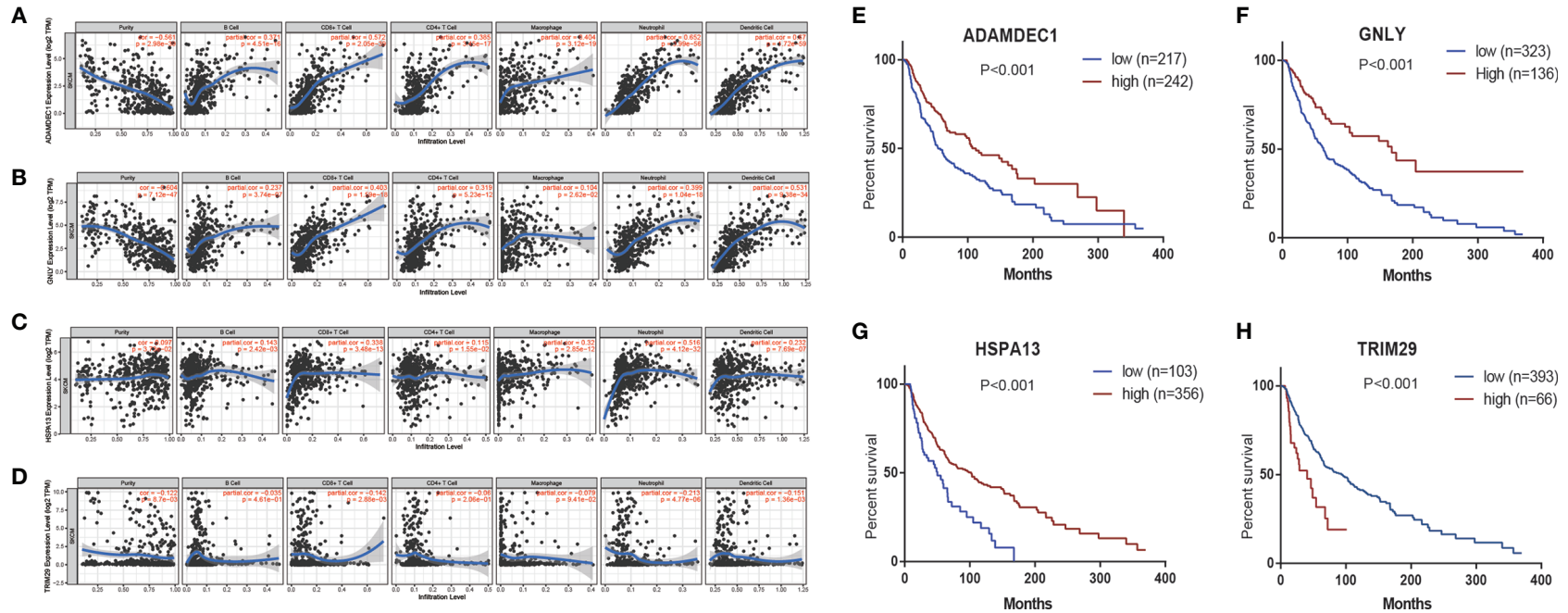


FIGURE 7 | The correlation between prognostic genes expression and immune cell infiltration in CM (TIMER database). The correlation between the abundance of immune cell and the expression of **(A)** ADAMDEC1; **(B)** GNLY; **(C)** HSPA13; **(D)** TRIM29. Prognostic values of **(E)** ADAMDEC1, **(F)** GNLY, **(G)** HSPA13, **(H)** TRIM29 in TCGA CM.

cells or cells infected by pathogens. GNLY can also activate antigen-presenting cells through TLR4 (24). Multiple publications have confirmed the anti-tumor activity of GNLY (25–29). Ya-Wen reported that the serum level of GNLY was negatively correlated with the proliferation of transplanted tumor cells in HIS mice (30). All gene in this risk model are firstly studied in cutaneous melanoma.

To sum up, our research results indicate that the four-gene prognostic model is a reliable tool for predicting the overall survival of CM, it may be useful for guiding therapeutic strategies to improve the clinical outcome of melanoma patients. The low-risk group should avoid some unnecessary treatment to reduced drug toxicities, and high-risk group can receive other intensive treatment. For clinical application, more clinical studies are needed to further verify the prognostic and predictive significance of the risk score model.

CONCLUSIONS

In conclusion, the new risk score system functions well in predicting the prognosis and treatment response in CM patients, with the potential to optimize treatment options. More studies are needed to explore the biological function of

these four genes in CM progression and to further verify the prognostic value of the model for clinical practice.

DATA AVAILABILITY STATEMENT

The original contributions presented in the study are included in the article/supplementary material. Further inquiries can be directed to the corresponding author.

AUTHOR CONTRIBUTIONS

This work was carried out in collaboration with all authors. MW designed the theme of the article. XT wrote and XQ reviewed the article. All authors contributed to the article and approved the submitted version.

ACKNOWLEDGMENTS

We thank Yuhu Xin, Ping Zhang, and Na Wang for their support over the past years.

REFERENCES

- Carr S, Smith C, Wernberg J. Epidemiology and Risk Factors of Melanoma. *Surg Clin North Am* (2020) 100:1–12.
- Rebecca VW, Somasundaram R, Herlyn M. Pre-clinical modeling of cutaneous melanoma. *Nat Commun* (2020) 11(1):2858. doi: 10.1038/s41467-020-15546-9
- de Assis LVM, Moraes MN, Castrucci AML. The molecular clock in the skin, its functionality, and how it is disrupted in cutaneous melanoma: a new pharmacological target? *Cell Mol Life Sci* (2019) 76(19):3801–26. doi: 10.1007/s00018-019-03183-5
- Siegel RL, Miller KD, Jemal A. Cancer statistics, 2015. *CA Cancer J Clin* (2015) 65(1):5–29. doi: 10.3322/caac.21254
- Hartman RI, Lin JY. Cutaneous Melanoma-A Review in Detection, Staging, and Management. *Hematol Oncol Clin North Am* (2019) 33(1):25–38. doi: 10.1016/j.hoc.2018.09.005
- Balch CM, Gershenwald JE, Soong SJ, Thompson JF, Atkins MB, Byrd DR, et al. Final version of 2009 AJCC melanoma staging and classification. *J Clin Oncol* (2009) 27(36):6199–206. doi: 10.1200/JCO.2009.23.4799
- Bertoli G, Cava C, Castiglioni I. MicroRNAs: New Biomarkers for Diagnosis, Prognosis, Therapy Prediction and Therapeutic Tools for Breast Cancer. *Theranostics* (2015) 5(10):1122–43. doi: 10.7150/thno.11543
- Sparano JA, Gray RJ, Makower DF, Pritchard KI, Albain KS, Hayes DF, et al. Adjuvant Chemotherapy Guided by a 21-Gene Expression Assay in Breast Cancer. *N Engl J Med* (2018) 379(2):111–21. doi: 10.1056/NEJMoa1804710
- Daoud AZ, Mulholland EJ, Cole G, McCarthy HO. MicroRNAs in Pancreatic Cancer: biomarkers, prognostic, and therapeutic modulators. *BMC Cancer* (2019) 19(1):1130. doi: 10.1186/s12885-019-6284-y
- Albain KS, Barlow WE, Shak S, Hortobagyi GN, Livingston RB, Yeh IT, et al. Prognostic and predictive value of the 21-gene recurrence score assay in postmenopausal women with node-positive, oestrogen-receptor-positive breast cancer on chemotherapy: a retrospective analysis of a randomised trial. *Lancet Oncol* (2010) 11(1):55–65. doi: 10.1016/S1470-2045(09)70314-6
- Ruan GT, Gong YZ, Zhu LC, Gao F, Liao XW, Wang XK, et al. The Perspective of Diagnostic and Prognostic Values of Lipoxigenases mRNA Expression in Colon Adenocarcinoma. *Onco Targets Ther* (2020) 13:9389–405. doi: 10.2147/OTT.S251965
- Gomez-Maldonado L, Tiana M, Roche O, Prado-Cabrero A, Jensen L, Fernandez-Barral A, et al. EFNA3 long noncoding RNAs induced by hypoxia promote metastatic dissemination. *Oncogene* (2015) 34(20):2609–20. doi: 10.1038/ncr.2014.200
- Spradling KD, McDaniel AE, Lohi J, Pilcher BK. Epsin 3 is a novel extracellular matrix-induced transcript specific to wounded epithelia. *J Biol Chem* (2001) 276(31):29257–67. doi: 10.1074/jbc.M101663200
- Schiano Lomoriello I, Giangreco G, Iavarone C, Tordonato C, Caldieri G, Serio G, et al. A self-sustaining endocytic-based loop promotes breast cancer plasticity leading to aggressiveness and pro-metastatic behavior. *Nat Commun* (2020) 11(1):3020. doi: 10.1038/s41467-020-16836-y
- Sigurdson AJ, Brenner AV, Roach JA, Goudeva L, Muller JA, Nerlich K, et al. Selected single-nucleotide polymorphisms in FOXE1, SERPINA5, FTO, EVPL, TICAM1 and SCARB1 are associated with papillary and follicular thyroid cancer risk: replication study in a German population. *Carcinogenesis* (2016) 37(7):677–84. doi: 10.1093/carcin/bgw047
- Fan H, Zhang S, Zhang Y, Liang W, Cao B. FERMT1 promotes gastric cancer progression by activating the NF-kappaB pathway and predicts poor prognosis. *Cancer Biol Ther* (2020) 21(9):815–25. doi: 10.1080/15384047.2020.1792218
- Pietras A, von Stedingk K, Lindgren D, Pahlman S, Axelson H. JAG2 induction in hypoxic tumor cells alters Notch signaling and enhances endothelial cell tube formation. *Mol Cancer Res* (2011) 9(5):626–36. doi: 10.1158/1541-7786.MCR-10-0508
- Takahashi T, Matsuda Y, Yamashita S, Hattori N, Kushima R, Lee YC, et al. Estimation of the fraction of cancer cells in a tumor DNA sample using DNA methylation. *PLoS One* (2013) 8(12):e82302. doi: 10.1371/journal.pone.0082302
- Hu JW, Yang ZF, Li J, Hu B, Luo CB, Zhu K, et al. TGM3 promotes epithelial-mesenchymal transition and hepatocellular carcinogenesis and predicts poor prognosis for patients after curative resection. *Dig Liver Dis* (2020) 52(6):668–76. doi: 10.1016/j.dld.2019.10.010
- Xing J, Weng L, Yuan B, Wang Z, Jia L, Jin R, et al. Identification of a role for TRIM29 in the control of innate immunity in the respiratory tract. *Nat Immunol* (2016) 17(12):1373–80. doi: 10.1038/ni.3580

21. Sun J, Zhang T, Cheng M, Hong L, Zhang C, Xie M, et al. TRIM29 facilitates the epithelial-to-mesenchymal transition and the progression of colorectal cancer via the activation of the Wnt/beta-catenin signaling pathway. *J Exp Clin Cancer Res* (2019) 38(1):104. doi: 10.1186/s13046-019-1098-y
22. Bates EE, Fridman WH, Mueller CG. The ADAMDEC1 (decysin) gene structure: evolution by duplication in a metalloprotease gene cluster on chromosome 8p12. *Immunogenetics* (2002) 54(2):96–105. doi: 10.1007/s00251-002-0430-3
23. Vujaklija DV, Gulic T, Susic S, Nagata K, Ogawa K, Laskarin G, et al. First trimester pregnancy decidual natural killer cells contain and spontaneously release high quantities of granulysin. *Am J Reprod Immunol* (2011) 66(5):363–72. doi: 10.1111/j.1600-0897.2011.01015.x
24. Tewary P, Yang D, de la Rosa G, Li Y, Finn MW, Krensky AM, et al. Granulysin activates antigen-presenting cells through TLR4 and acts as an immune alarmin. *Blood* (2010) 116(18):3465–74. doi: 10.1182/blood-2010-03-273953
25. Clayberger C, Krensky AM. Granulysin. *Curr Opin Immunol* (2003) 15(5):560–5. doi: 10.1016/S0952-7915(03)00097-9
26. Lin J, Huang Y, Zhang L, Tang W, Li X, Wang X, et al. Evaluation of serum granulysin as a potential biomarker for nasopharyngeal carcinoma. *Clin Chim Acta* (2016) 454:72–6. doi: 10.1016/j.cca.2015.12.035
27. Aporta A, Catalan E, Galan-Malo P, Ramirez-Labrada A, Perez M, Azaceta G, et al. Granulysin induces apoptotic cell death and cleavage of the autophagy regulator Atg5 in human hematological tumors. *Biochem Pharmacol* (2014) 87(3):410–23. doi: 10.1016/j.bcp.2013.11.004
28. Jiang W, Zhu D, Wang C, Zhu Y. An immune relevant signature for predicting prognoses and immunotherapeutic responses in patients with muscle-invasive bladder cancer (MIBC). *Cancer Med* (2020) 9(8):2774–90. doi: 10.1002/cam4.2942
29. Saini RV, Wilson C, Finn MW, Wang T, Krensky AM, Clayberger C. Granulysin delivered by cytotoxic cells damages endoplasmic reticulum and activates caspase-7 in target cells. *J Immunol* (2011) 186(6):3497–504. doi: 10.4049/jimmunol.1003409
30. Hsiao YW, Lai TC, Lin YH, Su CY, Lee JJ, Liao AT, et al. Granulysin expressed in a humanized mouse model induces apoptotic cell death and suppresses tumorigenicity. *Oncotarget* (2017) 8(48):83495–508. doi: 10.18632/oncotarget.11473

Conflict of Interest: The authors declare that the research was conducted in the absence of any commercial or financial relationships that could be construed as a potential conflict of interest.

Copyright © 2021 Tong, Qu and Wang. This is an open-access article distributed under the terms of the Creative Commons Attribution License (CC BY). The use, distribution or reproduction in other forums is permitted, provided the original author(s) and the copyright owner(s) are credited and that the original publication in this journal is cited, in accordance with accepted academic practice. No use, distribution or reproduction is permitted which does not comply with these terms.